

Effects of chain stiffness and shear flow on nanoparticle dispersion and distribution in ring polymer melts^{*}

Dan WANG, Feng-qing LI, Xiang-hong WANG, Shi-ben LI, Lin-li HE^{†‡}

Department of Physics, Wenzhou University, Wenzhou 320035, China

[†]E-mail: linlihe@wzu.edu.cn

Received Nov. 24, 2019; Revision accepted Feb. 23, 2020; Crosschecked Mar. 1, 2020

Abstract: The dispersion behavior and spatial distribution of nanoparticles (NPs) in ring polymer melts are explored by using molecular dynamics (MD) simulations. As polymer-NP interactions increase, three general categories of polymer-mediated NP organization are observed, namely, contact aggregation, bridging, and steric dispersion, consistent with the results of equivalent linear ones in previous studies. In the case of direct contact aggregation among NPs, the explicit aggregation-dispersion transition of NPs in ring polymer melts can be induced by increasing the chain stiffness or applying a steady shear flow. Results further indicate that NPs can achieve an optimal dispersed state with the appropriate chain stiffness and shear flow. Moreover, shear flow cannot only improve the dispersion of NPs in ring polymer melts but also control the spatial distribution of NPs into a well-ordered structure. This improvement becomes more evident under stronger polymer-NP interactions. The observed induced-dispersion or ordered distribution of NPs may provide efficient access to the design and manufacture of high-performance polymer nanocomposites (PNCs).

Key words: Ring polymer; Nanocomposites; Chain stiffness; Shear flow; Molecular dynamics (MD)

<https://doi.org/10.1631/jzus.A1900530>

CLC number: O631.2

1 Introduction

Composite materials are widely used in aerospace, national defense, transportation, sports, and other fields (Zhang JX et al., 2019; Zhang YD et al., 2019; Zheng et al., 2019) because of their excellent properties, especially their designability. The modifier is uniformly dispersed in the melt material through an appropriate preparation method to form a composite system containing nano-sized materials (Usuki et al., 1993; Chen et al., 2007; Jain et al., 2008; Wei et al., 2015). The most prominent composite

materials are polymer nanocomposites (PNCs) (Gu et al., 2019; He et al., 2019; Jiang et al., 2019; Ma Y et al., 2019; Zhu et al., 2019), which consist of mixtures of polymers as a continuous phase and organic/inorganic particles as a dispersed phase. The mechanical, optical, and electrical properties of PNCs can be significantly enhanced by adding nanoparticles (NPs) (Caseri, 2000; Zhu et al., 2001; Roca et al., 2009; Delcambre et al., 2010; Feng et al., 2012; Zuev and Ivanova, 2012). A typical example of such enhancement is the addition of carbon black to rubber to improve its strength and durability (Huber et al., 1996).

NP-NP interactions are naturally strong, whereas polymer-NP interactions are relatively weak. NPs and polymers are in a state of mutual dislike. Therefore, NPs cannot easily achieve good dispersion in polymer melts under natural conditions. An important issue is the improvement of the dispersion and spatial

[‡] Corresponding author

^{*} Project supported by the National Natural Science Foundation of China (Nos. 21674082 and 21973070) and the Natural Science Foundation of Zhejiang Province (No. LY19B040006), China

 ORCID: Lin-li HE, <https://orcid.org/0000-0001-9297-4379>

© Zhejiang University and Springer-Verlag GmbH Germany, part of Springer Nature 2020

distribution of NPs in polymer melts. This problem has caught the attention of many researchers, and has been extensively studied in experiments (Mackay et al., 2006; Bokobza, 2007; Vaia and Maguire, 2007; Ganesan et al., 2010), theories (Hooper and Schweizer, 2005, 2006), and computer simulations (Liu et al., 2008, 2011a, 2011b; Goswami and Sumpter, 2009; Shen et al., 2011; Chen et al., 2014). Bokobza (2007) improved the properties of a styrene-butadiene copolymer (modulus $\leq 45\%$; tensile length $\leq 70\%$) by addition of multi-wall carbon nanotubes, thus confirming that the ordered dispersion of carbon nanotubes throughout the material can remarkably enhance its mechanical properties. Vaia and Maguire (2007) found that the electrical and thermal conductivity of NP dispersions can be enhanced by studying their layered morphology outside their 3D and uniaxial alignment. Mackay et al. (2006) proved that thermodynamically stable dispersions of NPs into a polymeric liquid are enhanced for systems where the radius of gyration of the linear polymer is greater than the radius of the NP. Ganesan et al. (2010) incorporated graphene and graphene oxide in elastomeric matrixes. They proved that the formation of an oriented network of fillers can improve the gas permeability or mechanical properties in certain directions. Hooper and Schweizer (2005, 2006) theoretically proposed four aggregation and dispersion laws of PNCs: (1) contact aggregation, (2) dispersion, (3) close bridging of segmented horizontal particles, and (4) remote bridging, according to the interaction strength between NPs and polymer chains. Liu et al. (2008, 2011a, 2011b) used the molecular dynamics (MD) method to explore the effects of size, concentration, particle mass, chain length, and polymer-particle interactions on the diffusion of particles in linear polymer melts. They demonstrated that the interaction between NPs and polymers is weak in the phase of gathering, that good dispersion is achieved in moderate interaction, and that strong interaction leads to a bridged phase (one or two polymer chains between the two NPs). These findings verified the theory of Hooper et al. (2005) and presented important guiding significance for controlling the uniform dispersion and orderly arrangement of NPs in linear polymer melts. Chen et al. (2014) and Shen et al. (2011) also found that grafting polymer chains on the

surface of NPs is an effective means to control the dispersion degree of NPs. Goswami and Sumpter (2019) discussed the effects of polymer-filler interaction on the thermodynamic and dynamic properties of PNCs. They suggested that thermodynamic and dynamical responses can cause two types of “clustering transitions.”

In the polymer industry, processing polymer melts by applying an external force field is necessary to achieve some specific structures. Thus far, the application of shear flow to polymer melts is the most widely used approach to obtain specific structures. Several methods have been used to introduce shear flow into PNCs systems in previous MD simulations (Pryamitsyn and Ganesan, 2006; Chen et al., 2007, 2015; Kalra et al., 2010; Jaber et al., 2011). Kalra et al. (2010) found that shear flow can greatly alter the dynamics of NP aggregation in two ways: its effect on the NP diffusion coefficient and its effect on rupture-like deformation. Jaber et al. (2011) used MD simulations to determine the role that networks formed by fillers and polymers play in the rheology of PNCs. Their results indicated that the ability of fillers to maintain the network during shear results is enhanced. Chen et al. (2017) investigated the effect of steady shear on the ordering of string-like NP assemblies in functionalized polymer melts. They found that shear can induce 1D alignment to the NP strings and the emerging structures can remain stable after the cessation of shear.

Polymers with ring topology are very common (Benkova et al., 2016; Kruteva et al., 2017; Hossain et al., 2018; Narumi et al., 2018). However, studies on the ring polymer/NP composites are few. Most of these studies focus on linear polymer/NP composites (Hooper and Schweizer, 2005, 2006; Liu, 2008, 2011a, 2011b). Here, we propose an effective strategy to achieve good dispersion and spatial distribution of NPs in ring polymer melts. A ring polymer chain is formed by joining together the free ends of a linear polymer chain. The topological constraints of ring polymer chains decrease the conformational degrees of freedom, and this characteristic may be beneficial in improving the dispersion of NPs in ring polymer melts. Our study aims to combine chain stiffness and shear flow to improve the dispersion and spatial distribution of NPs in ring polymer melts.

2 Simulation method and models

In this study, the complex multi-factor interaction process in physics and mechanics was studied by computer simulation, which can make up for the shortcomings of theory in describing such complex phenomena, and can also overcome many difficulties or constraints encountered in experiments. As is well known, MD simulation is one of the most effective methods for predicting the structure, phase dynamics, and performance of PNCs under an equilibrium (Goswami and Sumpter, 2009; Feng et al., 2012; Zhao et al., 2017) or nonequilibrium (Pryamitsyn and Ganesan, 2006; Kalra et al., 2010; Chen et al., 2015) state, as its algorithm naturally contains real internal dynamics and can directly describe the dynamic behavior of the system.

In our MD simulation, a standard bead-spring model proposed by Kremer and Grest (1990) is used to describe a ring polymer chain. Each ring polymer chain consists of 20 spherical monomers with a bead diameter of σ and bead mass of m . Our system contains 850 polymer chains and 35 NPs with a diameter of 3σ . Thus, the mass of the NPs is 27 times that of the polymer bead. The interaction between the polymer adjacent bonded monomers is represented by a stiff finite extensible nonlinear elastic (FENE) potential (Kremer and Grest, 1990; Bennemann et al., 1999):

$$U_{\text{FENE}} = -0.5k R_0^2 \ln \left[1 - \left(\frac{r}{R_0} \right)^2 \right], \quad r < R_0, \quad (1)$$

where r is the distance between two neighbouring monomers, and $k=30\varepsilon/\sigma^2$, $R_0=1.5\sigma$. Our simulation does not focus on a specific polymer; thus, all calculated quantities are dimensionless. All quantities are reported in reduced units ($\varepsilon=1$, $\sigma=1$, and $m=1$ are the units of energy, length, and mass, respectively).

The stiffness of a polymer chain between adjacent bonds is described by the angle bending potential:

$$U_{\text{bending}} = K_b (1 + \cos\theta), \quad (2)$$

where θ is the angle between two consecutive bonds and the chain stiffness is controlled by varying the value of chain stiffness K_b .

The NPs are modeled as Lennard-Jones (LJ) spheres of radius R_n . Here, we use the modified LJ interaction to model the polymer-polymer, polymer-NP, and NP-NP interactions, as follows (Burgos-Mármol et al., 2017):

$$U_{ij} = \begin{cases} \infty, & 0 \leq r \leq R_{ij}, \\ 4\varepsilon_{ij} \left[\left(\frac{\sigma}{r-R_{ij}} \right)^{12} - \left(\frac{\sigma}{r-R_{ij}} \right)^6 \right] + U_{ij}^0 (R_{ij} + r_{ij}^c), & R_{ij} < r < R_{ij} + r_{ij}^c, \\ 0, & r \geq R_{ij} + r_{ij}^c, \end{cases} \quad (3)$$

where i and j refer to polymer chain monomer or NP bead, $r_{ij}^c = r - R_{EV}$, where the interaction is truncated and shifted to obtain zero energy and force. The energy parameter ε_{ij} represents the interaction between two chain monomers or NP beads. We offset the interaction range by R_{EV} to account for the excluded volume effects of different interaction sites. The pure attractive interactions between polymer-polymer are fixed at $\varepsilon_{pp}=1.0$ and R_{EV} becomes zero. The polymer-NP interactions are purely attractive, $R_{EV}=R_n-\sigma/2$, and $r_{ij}^c=2.5\sigma$. We can control the polymer-NP interactions by changing the value of ε_{np} . NP-NP pure repulsive interactions are fixed at $\varepsilon_{nn}=1.0$, with $R_{EV}=2R_n-\sigma$ and $r_{ij}^c=2^{1/6}\sigma$.

In our simulation system, we study the nonequilibrium distribution of NPs by applying a steady shear flow to ring polymer chains. Application of a steady shear flow follows the nonequilibrium molecular dynamics (NEMD) method originally proposed by Müller-Plath (Calderon and Ashurst, 2002). The shear viscosity connects a shear field with a flux of transverse linear momentum. In this reverse nonequilibrium method, the shear flow is a gradient of the fluid velocity along a special direction (Shan et al., 2018). In our simulation, we apply shear flow along the z direction. Thus, the velocity gradient generated in the x direction is expressed as $\partial v_z / \partial x$ or the shear rate $\dot{\gamma}$, as shown in Fig. 1a. L is the side length of simulation box. The momentum flux $j_x(p_z)$ can be expressed as follows (Müller-Plathe and Bordat, 2004):

$$j_x(p_z) = -\eta \frac{\partial v_z}{\partial x}, \quad (4)$$

where the proportionality coefficient η reflects the shear viscosity. The periodic simulation cell is subdivided into slabs along the x direction, where the beads inside the slab at $x=0$ and $x=L_x/2$ (L_x is the length of the box in the x direction) are propelled in the two opposite x directions. In this method, the velocity maintains a linear variance to ensure uniform momentum transfer efficiency across the system, as shown in Fig. 1b.

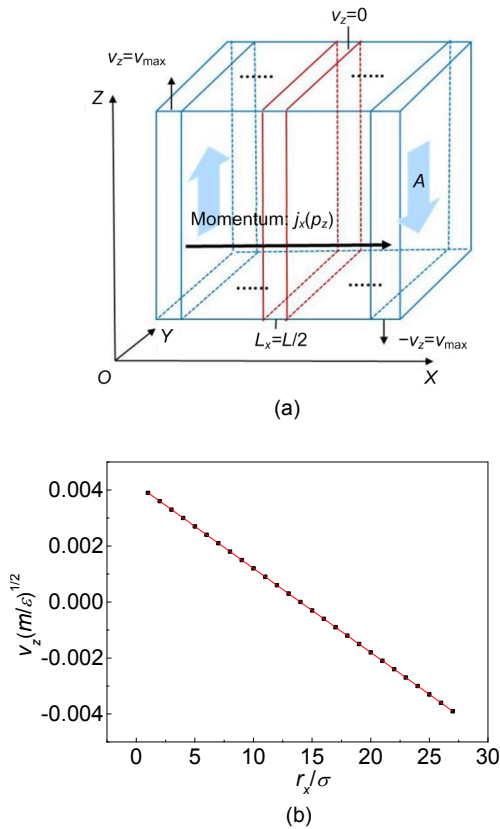


Fig. 1 Geometry of the nonequilibrium situation in simulation box (shear flow is applied in the z direction, where the velocity gradient is in the x direction, thereby resulting in a momentum flux $j_x(p_z)$ through the y - z plane of area A) (a); Example of a velocity profile in the simulation box with the parameters of $\varepsilon_{np}=0.5$, $K_b=0$, and $\dot{\gamma}=0.05$ (b)

All MD simulations are conducted using the large-scale atomic/molecular massively parallel simulator (LAMMPS) molecular dynamics package (Plimpton, 1995). The simulation box is set at $30\sigma \times 30\sigma \times 30\sigma$, and periodic boundary conditions are used in all three directions. Our MD simulations are

performed in an NVT canonical ensemble (particle number N , volume V , and temperature T are all unchanged) at a fixed temperature $T^*=1.0T$. All ring polymer chains and NPs are randomly placed and movable. In addition, the velocity-Verlet algorithm is used to integrate the equation of motions with time step $\Delta t=0.005\tau$, where the unit of time $\tau = \sqrt{\varepsilon / (m\sigma^2)}$.

3 Results and discussion

3.1 Chain stiffness effect

To investigate the dispersion of NPs in ring polymer melts, we initially change the polymer-NP interfacial strength from $\varepsilon_{np}=0.5$ to $\varepsilon_{np}=10.0$. We calculate the NP-NP pair radial distribution function (RDF) $g_{nn}(r)$ to display the dispersion and aggregation behavior of NPs in ring polymer melts, as shown in Fig. 2. The highest peak with a weak polymer-NP interaction of $\varepsilon_{np}=0.5$ appears at $r=3\sigma$, thereby suggesting that the NPs are in direct-contact state, as shown in the illustrations. The reason for this phenomenon is that the NP-NP interaction is stronger than the polymer-NP interaction, and NPs cannot easily disperse in polymer melts without any external force (Isaac et al., 2013; Patra and Singh, 2013), leading to NPs tending to aggregate naturally. When the polymer-NP interaction is increased to $\varepsilon_{np}=10.0$, the peak value is shifted to $r=5\sigma$. Because of the strong polymer-NP interaction, the polymer chains are sandwiched between two NPs, which can be referred to as the bridging state (Smith et al., 2003). When $\varepsilon_{np}=2.5$, no peak corresponds to the dispersion state. This result implies that good dispersion can be obtained at a moderate polymer-NP interfacial strength, similar to the results of previous studies on the distribution of NPs in linear polymer melts (Yan et al., 2010; Liu et al., 2011b). The dispersion of NPs in polymer melts greatly affects the performance of PNCs. Here, we focus on a weak polymer-NP interaction of $\varepsilon_{np}=0.5$ and vary the chain stiffness to promote the transition from NP-NP aggregation to dispersion in ring polymer melts.

Fig. 3a shows that the chain stiffness can significantly reduce the peak value of $g_{nn}(r)$. When $K_b=4$, the peak value of $g_{nn}(r)$ with weak chain stiffness

decreases evidently compared with that of fully flexible rings, thereby indicating that the system is very sensitive to the chain stiffness K_b . Furthermore, the peak value of $g_{nn}(r)$ drops sharply as the chain stiffness K_b further increases. When $K_b=100$, the curve of $g_{nn}(r)$ has almost no peak value. With increasing K_b , the conformation of ring polymers changes from a completely flexible chain into a planar rigid ring. Moreover, the repulsive volume between ring polymer chains and NPs increases, thereby increasing the area of direct contact between the polymer and the NPs, which helps in the dispersion of the latter (Chen et al., 2019). This result is different from that of the dispersion of NPs in linear polymer melts studied by Burgos-Mármol et al. (2017). They believed that when the polymer-NP interaction is low, the increase of chain stiffness makes the configuration of the linear chain change from anisotropic to isotropic, enhancing the aggregation between polymers and hindering the dispersion of NPs. On the contrary, the flexible chain can better adapt to package and disperse NPs in the polymer matrix (Burgos-Mármol et al., 2017). To further understand the dispersion degree of NPs in polymer melts, we calculate the average distance $\langle d \rangle_{nn}$ between NPs. As shown in Fig. 3b, the average distance $\langle d \rangle_{nn}$ between NPs generally increases as chain stiffness is increased from $K_b=0$ to $K_b=30$ and then basically remains at approximately 20σ with further increasing K_b . This result also proves that increasing the chain stiffness can induce the transition from NP-NP aggregation to dispersion in the ring polymer melts.

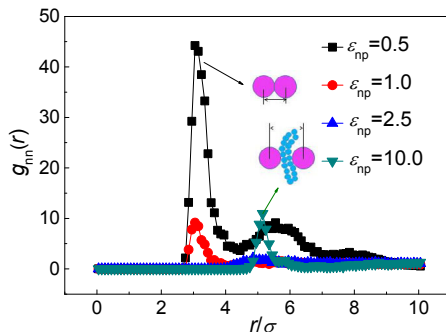


Fig. 2 NP-NP pair RDF $g_{nn}(r)$ for different polymer-NP interactions ϵ_{np} . NPs and polymer chains are shown in large balls and small beads, respectively

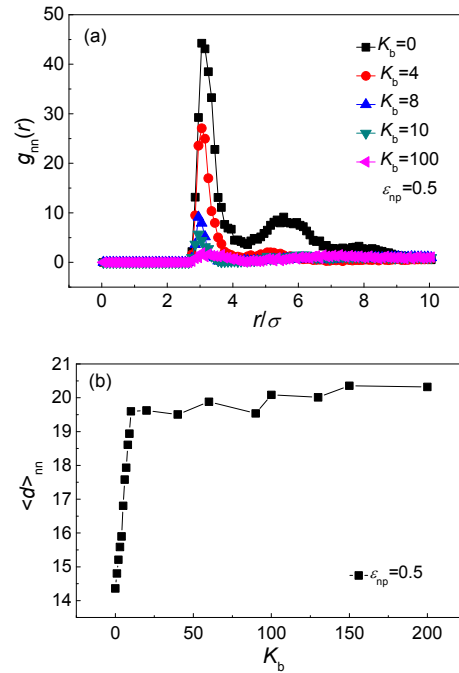


Fig. 3 NP-NP pair RDF $g_{nn}(r)$ for different chain stiffness K_b (a); NP-NP pair average distance $\langle d \rangle_{nn}$ for different chain stiffness K_b (b)

The distribution of polymer chains around NPs, $g_{np}(r)$, is calculated to investigate the conformation of ring polymers around NPs. As shown in Fig. 4a, the value of $g_{np}(r)$ at $r=2\sigma$ is significantly lower than 1.0 for $K_b=0$ and partly higher than 1.0 for $K_b=4$, and, especially, $K_b=100$. It indicates that the number of polymer monomers around an NP bead increases significantly when the chain stiffness K_b increases. NPs are forced to separate and enter into the semiflexible or planar rigid rings. This result is similar to the studies by Song et al. (2018), which investigated the adsorption behavior of linear polymer chains around NPs. Because of the different chain configuration and particle density, we obtained different values for RDF $g_{np}(r)$ compared with that of Song et al. (2018). The aggregation-dispersion transition induced by chain topological constraints is displayed clearly in Fig. 4b, which shows that increasing the chain stiffness can effectively improve the contact between polymer chains and NPs. Eq. (2) also indicates that, when K_b increases, the bending energy $U_{bending}$ of the ring polymer chains increases, thereby weakening the NP-NP interaction and further enriching NPs near the semiflexible ring polymer to achieve a dispersion state. As a result, increasing the

ring polymer chain stiffness can disperse NPs but not control their spatial arrangement.

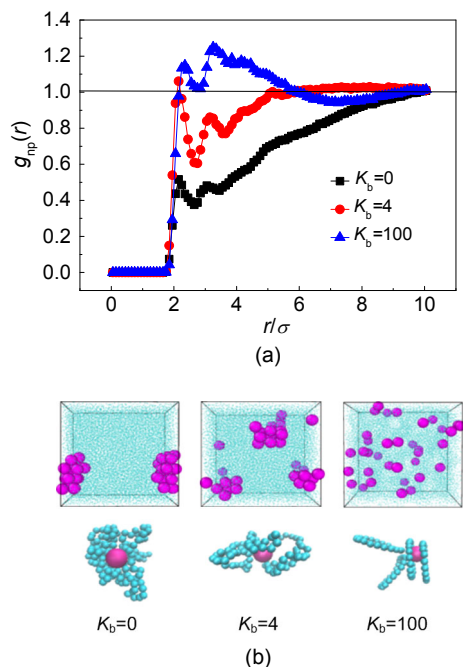


Fig. 4 Polymer-NP pair RDF $g_{np}(r)$ for different chain stiffness K_b (a); Corresponding snapshots and conformations of ring polymers adsorbed on the same NP (b)

3.2 Shear effect

Most PNC materials require NPs with good dispersion and an ordered arrangement in polymer melts. We apply the steady shear flow on ring polymers to improve the ordered arrangement of NPs. The radial RDF $g_{nn}(r)$ with different shear rates $\dot{\gamma}$ is shown in Fig. 5. The peak value of $g_{nn}(r)$ drops evidently with increasing shear strength $\dot{\gamma}$. The figure shows that polymer chains are stretched in the direction of shear flow. Therefore, the spatial distribution of NPs is affected directionally by the shear flow because of the strength of the polymer-NP interaction. This phenomenon is consistent with the studies of (Chen et al., 2017), which focused on the string-like NPs in a functionalized polymer matrix. They found that the shear can induce the string-like NPs into a 1D alignment arrangement. Fig. 6 shows the snapshots of polymer-NP melts with increasing shear rate $\dot{\gamma}$. A spherical aggregation of NPs exists when shear flow is absent. As $\dot{\gamma}$ increases from 0 to 0.05, the spherical aggregation of NPs is scattered and tends to disperse.

Figs. 6d and 6e correspond to the polymer-NP melts at $\dot{\gamma}=0.05$ displayed in the x - z and y - z planes, respectively. Fig. 6d shows a similar phenomenon of layered NPs in the x direction with good dispersion (Fig. 6e).

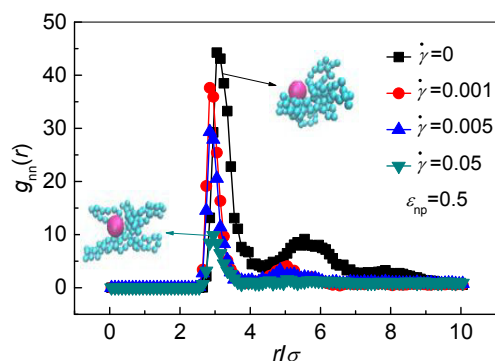


Fig. 5 NP-NP pair RDF $g_{nn}(r)$ for different shear rates $\dot{\gamma}$. The insets show the conformations of ring polymers adsorbed on the same NP

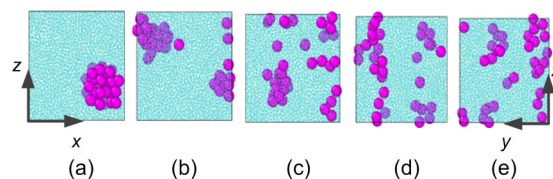


Fig. 6 Snapshots of the simulation of polymer-NP melts under different shear rates $\dot{\gamma}$

(a) $\dot{\gamma}=0$; (b) $\dot{\gamma}=0.001$; (c) $\dot{\gamma}=0.005$; (d) and (e) $\dot{\gamma}=0.05$. (a)–(d) are in the x - z plane, and (e) is in the y - z plane. Here, the shear flow is applied in the z direction

3.3 Chain stiffness and shear effect

We consider the effects of the chain stiffness and steady shear flow together. Fig. 7 shows that the peak value of $g_{nn}(r)$ dramatically decreases under either increasing the chain stiffness or applying shear flow alone. For example, when $K_b=4$ and $\dot{\gamma}=0.05$, the curve of $g_{nn}(r)$ has no peak, indicating the good dispersion of NPs. Therefore, good dispersion of NPs in ring polymer melts can be effectively induced by considering the chain stiffness and shear flow together. Compared with the results obtained at $K_b=0$ and $\dot{\gamma}=0.05$ shown in Fig. 6, we find that the spatial arrangement of NPs is very sensitive to the chain stiffness, especially in the case of weak polymer-NP

interactions. As chain stiffness increases from $K_b=0$ to $K_b=4$, the NPs exhibit better dispersion but lack a layered structure, as shown by the snapshot in Fig. 7. The density distributions of NPs in the x direction are displayed in Fig. 8. For $\varepsilon_{np}=0.5$ with $\dot{\gamma}=0$ and 0.05, the density distributions of NPs correspond to the snapshots in Figs. 6a and 6d. The two peaks in the curve of $\dot{\gamma}=0.05$ correspond to the layered NP structure, and only one peak in the curve of $\dot{\gamma}=0$ corresponds to the aggregated NP structure. However, an increase in chain stiffness would distinctly destroy the layered NP structure even under a strong shear flow, as shown Fig. 8c.

The effects of shear-stretched ring polymers on the spatial arrangement and distribution of NPs depend on the polymer-NP interactions. Here, we further increase the polymer-NP interaction from $\varepsilon_{np}=0.5$ to 10.0, as shown in Figs. 8b and 8d. Fig. 8b shows that NPs in shear-induced flexible ring polymer melts not only achieve good dispersion (illustration 1 in the x - z direction) but also form a well-layered structure (illustration 2 in the y - z direction). This result suggests that the shear-stretched polymers can arrange NPs along the shear flow. Then, under a strong shear of $\dot{\gamma}=0.05$, we further increase the chain stiffness from $K_b=0$ to 4 and 30, as shown in Fig. 8d. The chain stiffness does not weaken the layered arrangement of NPs but, instead, enhances the dispersion of NPs in ring polymer melts (illustration 2 in the y - z direction, shown in Fig. 8d). This result can be understood by considering that the increase in chain stiffness causes entropy depletion interactions between a pair of NPs to change from attractive to repulsive (Deng et al., 2016).

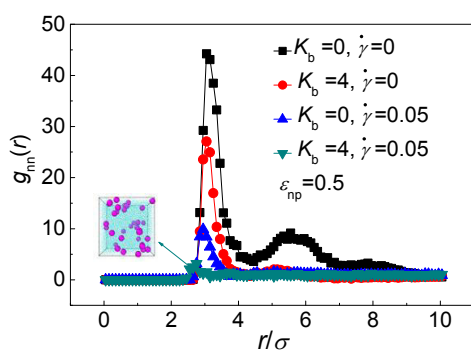


Fig. 7 NP-NP pair RDF $g_{nn}(r)$ for different chain stiffness K_b and shear rate $\dot{\gamma}$

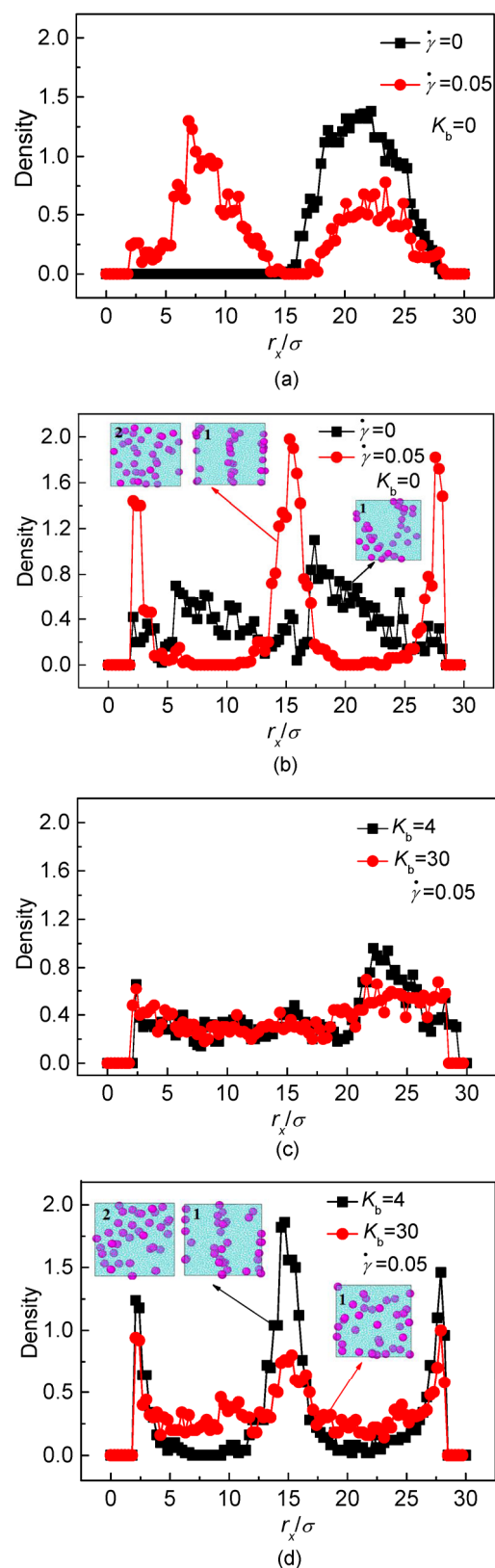


Fig. 8 Density distribution of NPs in the x direction (a) and (c) $\varepsilon_{np}=0.5$; (b) and (d) $\varepsilon_{np}=10.0$

4 Conclusions

We study the influence of chain stiffness and shear flow on the dispersion and spatial distribution of NPs in ring polymer melts using MD simulations. Direct contact aggregation among NPs occurs under very weak polymer-NP interactions. A transition from NPs aggregated state to dispersed state can be induced by increasing the ring chain stiffness or applying the shear strength. On the one hand, increasing the chain stiffness can produce well-dispersed NPs in ring polymer melts. NPs are wrapped by semiflexible (or rod-like) ring polymers, which effectively avoid NP aggregation and promote NP dispersion. On the other hand, with increasing shear strength, aggregated NPs also tend to be dispersed due to competition among polymer-NP interactions, NP-NP interactions, and shear flow. Because the polymer-NP interaction is strong, the spatial distribution of NPs is well ordered and well dispersed. The well-ordered structure is gradually disturbed by the increase of chain stiffness when shear flow and chain stiffness are considered at the same time in polymer chains. We combine chain stiffness and shear flow to effectively realize good dispersion and spatial distribution of NPs in ring polymer melts.

Contributors

Lin-li HE designed the research. Dan WANG and Feng-qing LI processed the corresponding data and wrote the first draft of the manuscript. Xiang-hong WANG and Shi-ben LI helped to organize the manuscript. Lin-li HE revised and edited the final version.

Conflict of interest

Dan WANG, Feng-qing LI, Xiang-hong WANG, Shi-ben LI, and Lin-li HE declare that they have no conflict of interest.

References

Benkova Z, Namer P, Cifra P, 2016. Comparison of a stripe and slab confinement for ring and linear macromolecules in nanochannel. *Soft Matter*, 12(40):8425-8439. <https://doi.org/10.1039/c6sm01507g>

Bennemann C, Paul W, Baschnagel J, et al., 1999. Investigating the influence of different thermodynamic paths on the structural relaxation in a glass-forming polymer melt. *Journal of Physics: Condensed Matter*, 11(10):2179-2192.

<https://doi.org/10.1088/0953-8984/11/10/005>

Bokobza L, 2007. Multiwall carbon nanotube elastomeric composites: a review. *Polymer*, 48(17):4907-4920. <https://doi.org/10.1016/j.polymer.2007.06.046>

Burgos-Mármol JJ, Álvarez-Machancoses Ó, Patti A, 2017. Modeling the effect of polymer chain stiffness on the behavior of polymer nanocomposites. *The Journal of Physical Chemistry B*, 121(25):6245-6256. <https://doi.org/10.1021/acs.jpcc.7b02502>

Calderon CP, Ashurst WT, 2002. Comment on "reversing the perturbation in nonequilibrium molecular dynamics: an easy way to calculate the shear viscosity of fluids". *Physical Review E*, 66(1):013201. <https://doi.org/10.1103/PhysRevE.59.4894>

Casari W, 2000. Nanocomposites of polymers and metals or semiconductors: historical background and optical properties. *Macromolecular Rapid Communications*, 21(11):705-722. [https://doi.org/10.1002/1521-3927\(20000701\)21:11<705::aid-marc705>3.0.co;2-3](https://doi.org/10.1002/1521-3927(20000701)21:11<705::aid-marc705>3.0.co;2-3)

Chen RJ, Poling-Skutvik R, Howard MP, et al., 2019. Influence of polymer flexibility on nanoparticle dynamics in semidilute solutions. *Soft Matter*, 15(6):1260-1268. <https://doi.org/10.1039/C8SM01834K>

Chen WD, Li YQ, Zhao HC, et al., 2015. Conformations and dynamics of single flexible ring polymers in simple shear flow. *Polymer*, 64:93-99. <https://doi.org/10.1016/j.polymer.2015.03.034>

Chen XY, Carbone P, Cavalcanti WL, et al., 2007. Viscosity and structural alteration of a coarse-grained model of polystyrene under steady shear flow studied by reverse nonequilibrium molecular dynamics. *Macromolecules*, 40(22):8087-8095. <https://doi.org/10.1021/ma0707178>

Chen YL, Li ZW, Wen SP, et al., 2014. Molecular simulation study of role of polymer-particle interactions in the strain-dependent viscoelasticity of elastomers (Payne effect). *The Journal of Chemical Physics*, 141(10):104901. <https://doi.org/10.1063/1.4894502>

Chen YL, Liu J, Li L, et al., 2017. Tailoring the alignment of string-like nanoparticle assemblies in a functionalized polymer matrix via steady shear. *RSC Advances*, 7(15):8898-8907. <https://doi.org/10.1039/C6RA28060A>

Delcambre SP, Riggelman RA, de Pablo JJ, et al., 2010. Mechanical properties of antiplasticized polymer nanostructures. *Soft Matter*, 6(11):2475-2483. <https://doi.org/10.1039/b926843j>

Deng ZY, Jiang YW, He LL, et al., 2016. Aggregation-dispersion transition for nanoparticles in semiflexible ring polymer nanocomposite melts. *The Journal of Physical Chemistry B*, 120(44):11574-11581. <https://doi.org/10.1021/acs.jpcc.6b07292>

- Feng YC, Zou H, Tian M, et al., 2012. Relationship between dispersion and conductivity of polymer nanocomposites: a molecular dynamics study. *The Journal of Physical Chemistry B*, 116(43):13081-13088.
<https://doi.org/10.1021/jp305815r>
- Ganesan V, Ellison CJ, Pryamitsyn V, 2010. Mean-field models of structure and dispersion of polymer-nanoparticle mixtures. *Soft Matter*, 6(17):4010-4025.
<https://doi.org/10.1039/b926992d>
- Goswami M, Sumpter BG, 2009. Effect of polymer-filler interaction strengths on the thermodynamic and dynamic properties of polymer nanocomposites. *The Journal of Chemical Physics*, 130(13):134910.
<https://doi.org/10.1063/1.3105336>
- Gu HB, Xu XJ, Dong MY, et al., 2019. Carbon nanospheres induced high negative permittivity in nanosilver-polydopamine meta-composites. *Carbon*, 147:550-558.
<https://doi.org/10.1016/j.carbon.2019.03.028>
- He YX, Chen QY, Liu H, et al., 2019. Friction and wear of MoO₃/Graphene oxide modified glass fiber reinforced epoxy nanocomposites. *Macromolecular Materials and Engineering*, 304(8):1900166.
<https://doi.org/10.1002/mame.201900166>
- Hooper JB, Schweizer KS, 2005. Contact aggregation, bridging, and steric stabilization in dense polymer-particle mixtures. *Macromolecules*, 38(21):8858-8869.
<https://doi.org/10.1021/ma051318k>
- Hooper JB, Schweizer KS, 2006. Theory of phase separation in polymer nanocomposites. *Macromolecules*, 39(15):5133-5142.
<https://doi.org/10.1021/ma060577m>
- Hossain MD, Reid JC, Lu DR, et al., 2018. Influence of constraints within a cyclic polymer on solution properties. *Biomacromolecules*, 19(2):616-625.
<https://doi.org/10.1021/acs.biomac.7b01690>
- Huber G, Vilgis TA, Heinrich G, 1996. Universal properties in the dynamical deformation of filled rubbers. *Journal of Physics: Condensed Matter*, 8(29):L409.
<https://doi.org/10.1088/0953-8984/8/29/003>
- Isaac R, Gobalakrishnan S, Rajan G, et al., 2013. An overview of facile green biogenic synthetic routes and applications of platinum nanoparticles. *Advanced Science*, 5(8):763-770.
<https://doi.org/10.1166/asem.2013.1377>
- Jaber E, Luo HB, Li WT, et al., 2011. Network formation in polymer nanocomposites under shear. *Soft Matter*, 7(8):3852-3860.
<https://doi.org/10.1039/c0sm00990c>
- Jain SC, Goossens JGP, Peters GWM, et al., 2008. Strong decrease in viscosity of nanoparticle-filled polymer melts through selective adsorption. *Soft Matter*, 4(9):1848-1854.
<https://doi.org/10.1039/b802905a>
- Jiang DW, Wang Y, Li BJ, et al., 2019. Flexible sandwich structural strain sensor based on silver nanowires decorated with self-healing substrate. *Macromolecular Materials and Engineering*, 304(7):1900074.
<https://doi.org/10.1002/mame.201900074>
- Kalra V, Escobedo F, Joo YL, 2010. Effect of shear on nanoparticle dispersion in polymer melts: a coarse-grained molecular dynamics study. *The Journal of Chemical Physics*, 132(2):024901.
<https://doi.org/10.1063/1.3277671>
- Kremer K, Grest GS, 1990. Dynamics of entangled linear polymer melts: a molecular-dynamics simulation. *The Journal of Chemical Physics*, 92(8):5057-5086.
<https://doi.org/10.1063/1.458541>
- Kruteva M, Allgaier J, Richter D, 2017. Direct observation of two distinct diffusive modes for polymer rings in linear polymer matrices by Pulsed Field Gradient (PFG) NMR. *Macromolecules*, 50(23):9482-9493.
<https://doi.org/10.1021/acs.macromol.7b01850>
- Liu J, Cao DP, Zhang LQ, 2008. Molecular dynamics study on nanoparticle diffusion in polymer melts: a test of the Stokes-Einstein law. *The Journal of Physical Chemistry C*, 112(17):6653-6661.
<https://doi.org/10.1021/jp800474t>
- Liu J, Gao YY, Cao DP, et al., 2011a. Nanoparticle dispersion and aggregation in polymer nanocomposites: insights from molecular dynamics simulation. *Langmuir*, 27(12):7926-7933.
<https://doi.org/10.1021/la201073m>
- Liu J, Wu Y, Shen JX, et al., 2011b. Polymer-nanoparticle interfacial behavior revisited: a molecular dynamics study. *Physical Chemistry Chemical Physics*, 13(28):13058-13069.
<https://doi.org/10.1039/c0cp02952a>
- Ma LC, Zhu YY, Feng PF, et al., 2019. Reinforcing carbon fiber epoxy composites with triazine derivatives functionalized graphene oxide modified sizing agent. *Composites Part B: Engineering*, 176:107078.
<https://doi.org/10.1016/j.compositesb.2019.107078>
- Ma Y, Hou CP, Zhang HP, et al., 2019. Three-dimensional core-shell Fe₃O₄/Polyaniline coaxial heterogeneous nanonets: preparation and high performance supercapacitor electrodes. *Electrochimica Acta*, 315:114-123.
<https://doi.org/10.1016/j.electacta.2019.05.073>
- Mackay ME, Tuteja A, Duxbury PM, et al., 2006. General strategies for nanoparticle dispersion. *Science*, 311(5768):1740-1743.
<https://doi.org/10.1126/science.1122225>
- Müller-Plathe F, Bordat P, 2004. Reverse non-equilibrium molecular dynamics. In: Karttunen M, Lukkarinen A, Vattulainen I (Eds.), *Novel Methods in Soft Matter Simulations*. Springer, Berlin, Germany, p.310-326.
https://doi.org/10.1007/978-3-540-39895-0_10
- Narumi A, Kobayashi T, Yamada M, et al., 2018. Ring-expansion/contraction radical crossover reactions of

- cyclic alkoxyamines: a mechanism for ring expansion-controlled radical polymerization. *Polymers*, 10(6):638. <https://doi.org/10.3390/polym10060638>
- Patra TK, Singh JK, 2013. Coarse-grain molecular dynamics simulations of nanoparticle-polymer melt: dispersion vs. agglomeration. *The Journal of Chemical Physics*, 138(14):144901. <https://doi.org/10.1063/1.4799265>
- Plimpton S, 1995. Fast parallel algorithms for short-range molecular dynamics. *Journal of Computational Physics*, 117(1):1-19. <https://doi.org/10.1006/jcph.1995.1039>
- Pryamitsyn V, Ganesan V, 2006. Mechanisms of steady-shear rheology in polymer-nanoparticle composites. *Journal of Rheology*, 50(5):655-683. <https://doi.org/10.1122/1.2234483>
- Roca AG, Veintemillas-Verdaguer S, Port M, et al., 2009. Effect of nanoparticle and aggregate size on the relaxometric properties of MR contrast agents based on high quality magnetite nanoparticles. *The Journal of Physical Chemistry B*, 113(19):7033-7039. <https://doi.org/10.1021/jp807820s>
- Shan Y, Wang XH, Ji YY, et al., 2018. Self-assembly of phospholipid molecules in solutions under shear flows: microstructures and phase diagrams. *The Journal of Chemical Physics*, 149(24):244901. <https://doi.org/10.1063/1.5056229>
- Shen JX, Liu J, Gao YY, et al., 2011. Revisiting the dispersion mechanism of grafted nanoparticles in polymer matrix: a detailed molecular dynamics simulation. *Langmuir*, 27(24):15213-15222. <https://doi.org/10.1021/la203182u>
- Smith JS, Bedrov D, Smith GD, 2003. A molecular dynamics simulation study of nanoparticle interactions in a model polymer-nanoparticle composite. *Composites Science and Technology*, 63(11):1599-1605. [https://doi.org/10.1016/s0266-3538\(03\)00061-7](https://doi.org/10.1016/s0266-3538(03)00061-7)
- Song QL, Ji YY, Li SB, et al., 2018. Adsorption behavior of polymer chain with different topology structure at the polymer-nanoparticle interface. *Polymers*, 10(6):590. <https://doi.org/10.3390/polym10060590>
- Usuki A, Kojima Y, Kawasumi M, et al., 1993. Synthesis of nylon 6-clay hybrid. *Journal of Materials Research*, 8(5):1179-1184. <https://doi.org/10.1557/JMR.1993.1179>
- Vaia RA, Maguire JF, 2007. Polymer nanocomposites with prescribed morphology: going beyond nanoparticle-filled polymers. *Chemistry of Materials*, 19(11):2736-2751. <https://doi.org/10.1021/cm062693>
- Wei ZY, Hou YQ, Ning NY, et al., 2015. Theoretical insight into dispersion of silica nanoparticles in polymer melts. *The Journal of Physical Chemistry B*, 119(30):9940-9948. <https://doi.org/10.1021/acs.jpcc.5b01399>
- Yan LT, Popp N, Ghosh SK, et al., 2010. Self-assembly of Janus nanoparticles in diblock copolymers. *ACS Nano*, 4(2):913-920. <https://doi.org/10.1021/nn901739v>
- Zhang JX, Zhang WR, Wei LP, et al., 2019. Alternating multilayer structural epoxy composite coating for corrosion protection of steel. *Macromolecular Materials and Engineering*, 304(12):1900374. <https://doi.org/10.1002/mame.201900374>
- Zhang YD, An YF, Wu LY, et al., 2019. Metal-free energy storage systems: combining batteries with capacitors based on a methylene blue functionalized graphene cathode. *Journal of Materials Chemistry A*, 7(34):19668-19675. <https://doi.org/10.1039/c9ta06734e>
- Zhao JB, Wu LL, Zhan CX, et al., 2017. Overview of polymer nanocomposites: computer simulation understanding of physical properties. *Polymer*, 133:272-287. <https://doi.org/10.1016/j.polymer.2017.10.035>
- Zheng YW, Chen L, Wang XY, et al., 2019. Modification of renewable cardanol onto carbon fiber for the improved interfacial properties of advanced polymer composites. *Polymers*, 12(1):45. <https://doi.org/10.3390/polym12010045>
- Zhu GY, Cui XK, Zhang Y, et al., 2019. Poly (vinyl butyral)/graphene oxide/poly (methylhydrosiloxane) nanocomposite coating for improved aluminum alloy anticorrosion. *Polymer*, 172:415-422. <https://doi.org/10.1016/j.polymer.2019.03.056>
- Zhu J, Uhl FM, Morgan AB, et al., 2001. Studies on the mechanism by which the formation of nanocomposites enhances thermal stability. *Chemistry of Materials*, 13(12):4649-4654. <https://doi.org/10.1021/cm010451y>
- Zuev VV, Ivanova YG, 2012. Mechanical and electrical properties of polyamide-6-based nanocomposites reinforced by fulleroid fillers. *Polymer Engineering & Science*, 52(6):1206-1211. <https://doi.org/10.1002/pen.22188>

中文概要

题目: 链刚性和剪切场对环形聚合物熔体中纳米颗粒分散和空间分布的影响

目的: 一般情况下, 纳米粒子在环形聚合物熔体中处于聚集状态。本文通过增加链刚性或施加稳定的剪切场来诱导纳米粒子在环形聚合物熔体中的聚集-分散转变, 使环形聚合物中的纳米粒子达到最优的分散状态。

创新点: 同时改变链刚性和剪切场强度, 诱导纳米粒子在分散的同时进行有序排列。

方 法: 利用分子动力学模拟方法, 研究纳米粒子在环形聚合物熔体中的分散和空间分布。

结 论: 1. 在较弱的高分子/纳米粒子 (polymer-NP) 相互作用力下, 增加环链的刚性或施加剪切场, 可以诱导纳米粒子 (NPs) 从聚集态向分散态过渡。2. 增加链的刚性可以提高 NPs 在环形聚合物熔体中的分散度; NPs 被半刚性 (或棒状) 环形聚合物链包裹, 有效地避免了 NPs 间的聚集, 促使其分散。3. 随着剪切场强度的增加, 聚集的 NPs 也

会因 polymer-NP 相互作用、NP-NP 相互作用以及剪切场之间的竞争而趋于分散; 由于 polymer-NP 相互作用强, 所以 NPs 的空间分布具有良好的有序性和分散性。4. 同时考虑剪切场和链刚性, 可有效提高 NPs 在环形聚合物熔体中的分散度和空间分布, 而链刚性的增加干扰了 NPs 的有序结构。

关键词: 环形聚合物; 纳米复合材料; 链刚性; 剪切场; 分子动力学